Agricultural Water Management 163 (2016) 332–343

Contents lists available at ScienceDirect

Agricultural Water Management

journal homepage: www.elsevier.com/locate/agwat

Evaluating the impacts of crop rotations on groundwater storage and recharge in an agricultural watershed

Abdullah O. Dakhlalla[a,*], Prem B. Parajuli[a], Ying Ouyang[b], Darrel W. Schmitz[c]

[a] Department of Agricultural and Biological Engineering, Mississippi State University, Mississippi State, MS 39762, USA
[b] USDA Forest Service, Mississippi State, USA
[c] Department of Geosciences, Mississippi State University, Mississippi State, USA

ARTICLE INFO

Article history:
Received 16 February 2015
Received in revised form
28 September 2015
Accepted 1 October 2015
Available online 28 October 2015

Keywords:
Groundwater
Watershed modeling
Crop rotations
Irrigation
SWAT

ABSTRACT

The Mississippi River Valley Alluvial Aquifer, which underlies the Big Sunflower River Watershed (BSRW), is the most heavily used aquifer in Mississippi. Because the aquifer is primarily used for irrigating crops such as corn, cotton, soybean, and rice, the water levels have been declining rapidly over the past few decades. The objectives of this study are to analyze the relationship and interactions between evapotranspiration and groundwater recharge rates in the BSRW, and model the effects of various crop rotation practices on groundwater storage and recharge.

The model performed well during the calibration period (R^2 = 0.53–0.68 and NSE = 0.49–0.66) and validation period (R^2 = 0.55–0.75 and NSE = 0.49–0.72) for daily streamflow, which was achieved by the SUFI-2 auto-calibration algorithm in the SWAT-CUP package. The model also performed well in simulating seasonal water table depth fluctuations during calibration (R^2 = 0.76 and NSE = 0.71) and validation (R^2 = 0.86 and NSE = 0.79). This study demonstrated a seasonal relationship between evapotranspiration and groundwater storage and recharge in the BSRW SWAT model. In general, groundwater storage decreased during the summer months while ET rates were high, and increased during the winter and spring months when ET rates were low. The crop rotation scenarios that include rice planting resulted in the lowest groundwater storage (down to −10.7%) compared to the baseline crop scenario, which is due to the high irrigation rates of the rice crop. However, the rice crop rotations resulted in the highest increases of groundwater recharge rates (up to +60.1%), likely because of the response to the deficiency of groundwater needed for irrigation as well as the limited water uptake by the rice crop. The crop rotations with corn and cotton resulted in the largest increases in groundwater storage (up to +27.2%), which is the result of the low irrigation rates as well as the short time period for irrigation applications. The results of this study are expected to aid farmers and watershed managers to conserve groundwater resources, but still maintain crop production.

1. Introduction

Research indicates that land use change is a prominent factor influencing the amount and movement of water in the hydrologic cycle, namely runoff, evapotranspiration, stream discharge, and groundwater flow (Batelis and Nalbantis, 2014; Khanal and Parajuli, 2013; Wang et al., 2013). These hydrological changes can result from alterations to surface roughness, soil characteristics, plant cover, and surface water storage (Parajuli et al., 2013; Thanapakpawin et al., 2006; Tuppad et al., 2010; Wild and Davis, 2009). While certain land use alteration strategies can alleviate the problems of surface water and groundwater scarcity, they can also cause adverse effects on the environment and exacerbate those problems (Foley et al., 2005; Lotze-Campen et al., 2008). Especially in agricultural areas, groundwater sources tend to be over extracted and exploited without any regard to employing any conservational or sustainable management practices (Fereres and Soriano, 2006). It is estimated that global groundwater reserves are being depleted very rapidly to meet the irrigation demand for crop production at a withdrawal rate of 545 km^3 per year, and this rate is expected to increase (Konikow, 2013; Siebert et al., 2010). Therefore, it becomes necessary to employ sustainable management practices to conserve groundwater in these areas while still maximizing crop production. Many field studies and modeling studies have attempted to quantify the effects of

* Corresponding author.
E-mail addresses: aod11@msstate.edu (A.O. Dakhlalla), youyang@fs.fed.us (Y. Ouyang), schmitz@geosci.msstate.edu (D.W. Schmitz).

http://dx.doi.org/10.1016/j.agwat.2015.10.001
0378-3774/

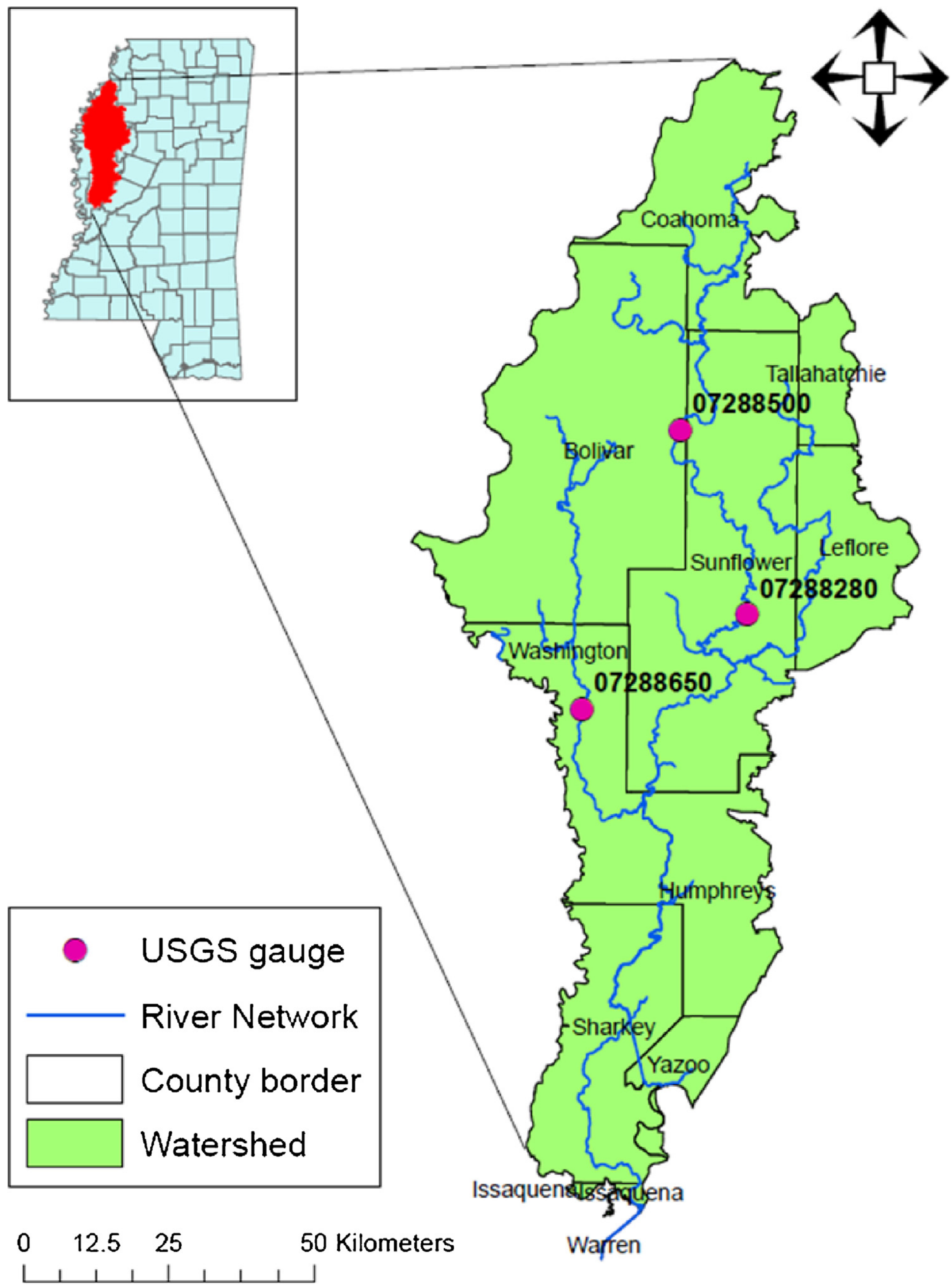

Fig. 1. Location of the Big Sunflower River Watershed (BSRW) in northwestern MS showing counties, river network, and USGS gauge stations.

changing land uses and soil characteristics on groundwater storage and flows. The results of a land use comparison study showed that groundwater recharge rates are much higher in an irrigated agricultural watershed (130–640 mm/yr) than in a non-irrigated agricultural watershed (9–32 mm/yr) (Scanlon et al., 2005). A study conducted in a watershed in Denmark found that converting grasslands to forests had a very small effect on groundwater recharge, while increased CO_2 caused considerable additional groundwater recharge within the watershed (Roosmalen et al., 2009). Huang et al. (2012) found that converting grassland to winter wheat over a 100-year period reduced groundwater recharge rates by up to 50%, which was attributed to the changes in evapotranspiration. A study that linked a vadose zone model and a saturated groundwater model for a watershed in south-western Australia found that recharge rates are higher in pasture land covers compared to areas with native vegetation (Dawes et al., 2012).

While the aforementioned studies evaluated the effects of land use change on groundwater flows, there are no studies specifically addressing the impacts of crop rotation practices on groundwater storage and recharge. This study will utilize the soil and water assessment tool (SWAT) to quantify the effects of crop rotations on groundwater storage and recharge.

In the past, SWAT has been used to calibrate and validate watershed models using groundwater table depths. However, it should be noted that the current version of SWAT does not print groundwater table depths, which makes verifying SWAT groundwater outputs somewhat challenging. For example, Vazquez-Amabile and Engel (2004) attempted to calibrate their watershed model with observed groundwater table depths using SWAT for three different soil types. They had to compute water table depths by using the soil input data and SWAT soil water output to predict fluctuations in the shallow aquifer, which is based on the DRAINMOD

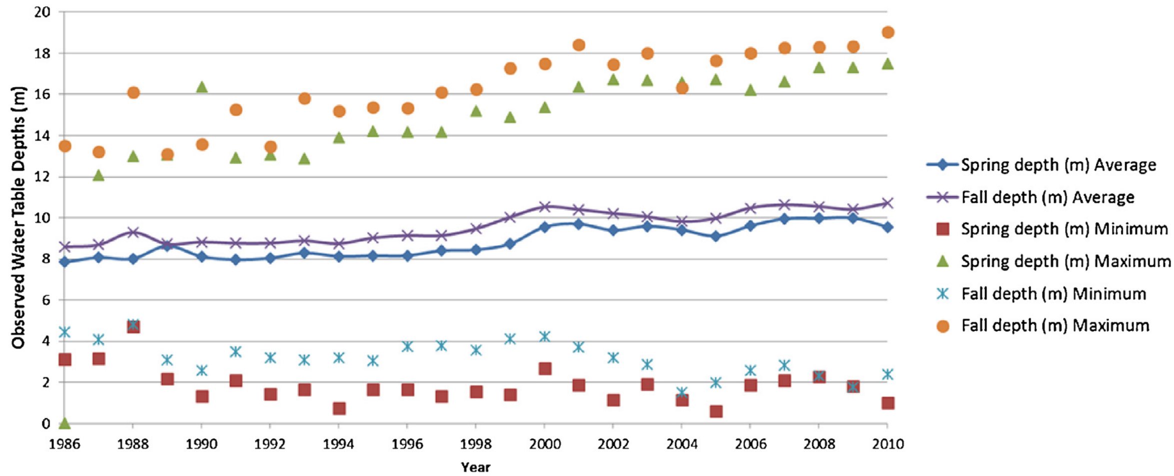

Fig. 2. The observed average, minimum, and maximum spring and fall water table depths from 1986 to 2010 in the BSRW.

model. While their model performed fairly well (R = 0.46–0.88 and Nash–Sutcliffe = −0.74–0.61), it did not accurately capture the monthly variation of groundwater table depth within the watershed. In subsequent studies conducted by Moriasi et al. (2009, 2011), a modified DRAINMOD approach was used to model water table depths based on the outputs of the SWAT model. This modified approach differs from the study conducted by Vazquez-Amabile and Engel (2004) in how the drainage volume is calculated and how the drainage volume is related to the water table depths (Moriasi et al., 2009). The authors reported that the DRAINMOD approach yielded better results than other water table depth algorithms used in SWAT, which are the SWAT-M and SWAT2005 approaches (Moriasi et al., 2009). Other SWAT groundwater modeling studies have integrated the SWAT model with MODFLOW, which is a distributed modular finite-difference groundwater flow model that is capable of simulating water table depths at the cell scale (Galbiati et al., 2006; Kim et al., 2008; Narula and Gosain, 2013; Perkins and Sophocleous, 1999; Sophocleous and Perkins, 2000). Typically, the integration process of SWAT and MODFLOW involves the SWAT calculated groundwater recharge rates at the hydrologic response unit (HRU) level being converted to the cell level, which is subsequently used as an input in MODFLOW (Kim et al., 2008). The MODFLOW model is then able to calculate groundwater related outputs such as water table depth, river-groundwater fluxes, and groundwater evapotranspiration (Kim et al., 2008). However, this integrative modeling method relies heavily on the HRU level groundwater recharge outputs from the SWAT model, which do not have any spatial location due to the nature of the construction of HRUs. Also, converting groundwater recharge rates at the HRU level to the cell level may not be feasible at the watershed scale due to expensive computational requirements. In another SWAT groundwater modeling study, it was possible to only use SWAT to calibrate and validate a model for changes in water table depths (Jayakody et al., 2013). This was accomplished by calculating evapotranspiration, percolation, and groundwater discharge to develop an empirical relationship with water table fluctuations that was able to predict 64% of the water table variation (Jayakody et al., 2013).

For this groundwater modeling study, SWAT was used to calibrate and validate a watershed scale model by comparing simulated seasonal variations of water table depths averaged at the sub-basin level to observed changes in water table depths. The objectives of this study are to (1) develop a calibrated and validated model using SWAT for streamflow and groundwater table depths in the Big Sunflower River Watershed (BSRW), (2) analyze the relationship and trends between evapotranspiration and groundwater recharge rates and (3) estimate the effects of various crop rotation practices on groundwater storage and recharge.

2. Methods

2.1. Watershed description

The BSRW is located in north-western Mississippi in an area of the lower Mississippi River alluvial plain known locally as the Delta (Fig. 1). The watershed covers 10,488 km^2 and contains heavy agricultural production for corn, soybean, cotton, and rice crops, which make up over 80% of the land use in the watershed (Parajuli et al., 2013). The BSRW has very little topographic relief and is bordered by the Mississippi River levee on the western boundary and the Bluff Hills on the eastern boundary (Coupe et al., 2012). The watershed contains mostly Alligator, Sharkey, Dowling, Forestdale, and Dundee soils, which have high clay and silt content (Table 1). These soils account for over 90% of the soil types in the watershed and are classified as NRCS hydrologic soil groups C and D, which allow for high runoff potential (Table 1).

Because of the low permeability of the soils, only small amounts of rainfall are allowed to seep through the soil horizons into the underlying Mississippi River Valley Alluvial Aquifer (MRVAA), which is the main source of irrigation for the watershed (Arthur, 2001). The MRVAA consists of mainly sand and gravel material from the quaternary age that generally reside around the center of the Mississippi River alluvium where the aquifer is at its thickest (Arthur, 2001). The underlying aquifers in the BSRW consist of the Forest Hill Formation, Cockfield Formation, and Sparta Sand aquifers, where the sediments of these aquifers consist of unconsolidated sand and clay beds of different thicknesses (Arthur, 2011). In the areas where clay beds of the underlying aquifers are in contact with the MRVAA, the hydraulic connection is weak or non-existent (Arthur, 2011). Conversely, in areas where the underlying sand beds are in contact with the MRVAA, there is usually a strong hydraulic connection (Arthur, 2001).

Groundwater in the MRVAA tends to flow southward where it follows the direction of the north to south slope of the alluvial plain, and it also flows laterally toward the Big Sunflower River which cuts through the center of the BSRW. The water table levels tend to be lowest in the center of the BSRW where the heaviest groundwater extraction occurs (Barlow and Clark, 2011). The water levels throughout the watershed are typically highest during the early spring season right before the growing season begins, and are

Table 1
List of soil types found in the BSRW that were obtained from the soil survey geographic (SSURGO) database.

Soil name	Percentage of watershed area	Hydrologic soil group	Clay content (%)	Silt content (%)	Sand content (%)
Alligator	28.36%	D	57.74	35.97	6.30
Sharkey	23.80%	D	64.02	29.38	6.60
Dowling	17.24%	D	61.75	30.55	7.70
Forestdale	14.79%	D	32.85	52.95	14.21
Dundee	8.83%	C	23.60	54.58	21.82
Commerce	1.69%	C	27.10	54.65	18.25
Tensas	1.11%	D	39.00	45.17	15.83
Dubbs	0.83%	B	18.83	46.30	34.87
Brittain	0.82%	D	32.00	52.97	15.03
Tunica	0.81%	D	42.83	33.42	23.75
Water	0.42%	D	N/A	N/A	N/A
Bosket (dubbs)	0.41%	B	18.83	44.90	36.27
Pearson	0.33%	C	23.17	58.37	18.47
Marsh	0.26%	B	31.00	33.60	35.40
Bosket (askew)	0.21%	C	20.50	36.27	43.23
No name	0.11%	B	31.00	33.60	35.40
Beulah	0.00%	B	9.83	20.40	69.77

lowest during the early fall. The observed average, minimum, and maximum spring and fall water table depths are shown in Fig. 2.

The MRVAA is capable of providing well yields of over 0.126 m^3/s for irrigation use, and the storage of the alluvial aquifer has been depleting at an exponential rate since the 1970's (Arthur, 2001; Clark and Hart, 2009; Konikow, 2013). As of March 2014, there have been almost 22,000 groundwater use permits issued within the Delta region, and they account for more than 80% of all issued groundwater use permits in the state of Mississippi. The extraction of groundwater for irrigation in the Mississippi Delta has gone beyond recharge rates needed to refill the aquifer, thus proving to be unsustainable over time.

2.2. SWAT model description

SWAT is a semi-distributed watershed scale model that predicts the impacts of climate change and management decisions on water and pollutant yields from large watersheds (Arnold et al., 1998). The watershed modeling tool delineates the watershed into sub-basins, which is then further divided into hydrological response units (HRUs). Each HRU consists of a unique combination of land use, soil, and slope. The user can customize each HRU to contain specific management practices as well as various parameters that govern surface water movement, groundwater movement, erosion processes, and pollutant transport (Neitsch et al., 2011). The water budget is calculated at the HRU level, which consists of precipitation, surface runoff, evapotranspiration, infiltration, and groundwater recharge (Neitsch et al., 2011). For this study, ArcSWAT 2012 was used to develop the BSRW model, which is an ArcGIS extension and graphical user input interface.

SWAT has two main reserves for groundwater storage, which are the shallow aquifer and the deep aquifer (Neitsch et al., 2011). In the model, the shallow aquifer is unconfined and the deep aquifer is confined. Water that enters the shallow aquifer from the top soil layers can either contribute to baseflow or percolate to the deep aquifer. Water stored in the shallow aquifer can also move upward to the overlying unsaturated zone by either evaporation or plant root uptake, which is termed in the SWAT model as "revap". Water in the shallow and deep aquifers can also be removed via groundwater pumping used for irrigation. The overall equation used to calculate the storage of groundwater in the shallow aquifer during each time step is presented in Eq. (1):

$$\mathrm{aq}_{\mathrm{sh},i} = \mathrm{aq}_{\mathrm{sh},i-1} + w_{\mathrm{rchrg,sh}} - Q_{\mathrm{gw}} - w_{\mathrm{revap}} - w_{\mathrm{pump,sh}} \quad (1)$$

where $\mathrm{aq}_{\mathrm{sh},i}$ is the amount of water stored in the shallow aquifer on day i (mm), $\mathrm{aq}_{\mathrm{sh},i-1}$ is the amount of water stored in the shallow aquifer on day $i-1$ (mm), $w_{\mathrm{rchrg,sh}}$ is the amount of recharge entering the shallow aquifer on day i (mm), Q_{gw} is the amount of baseflow entering the main channel on day i (mm), w_{revap} is the amount of revap moving into the soil zone on day i (mm), and $w_{\mathrm{pump,sh}}$ is the amount of water removed from the shallow aquifer for consumption on day i (mm) (Neitsch et al., 2011).

2.3. Model inputs

A 10 m × 10 m digital elevation model (DEM) was downloaded from United States Geological Survey (USGS) and used to delineate the BSRW into 32 sub-basins. The land use data were obtained from the USDA National Agricultural Statistics Service (NASS) in the form of a 30 m × 30 m cropland data layer. The soils data were obtained from the soil survey geographic (SSURGO) database from the Natural Resources Conservation Service (NRCS) in the form of a 30 m × 30 m raster layer. The cropland data layer and SSURGO raster dataset were used to divide the BSRW model sub-basins into 2209HRUs.

After the HRU generation, the climate data were incorporated in the model from various weather stations. Daily precipitation and temperature data were obtained from the USDA climatic database where the data was preformatted to use in SWAT. These climate data were derived from the National Oceanic and Atmospheric Administration (NOAA) which includes the Cooperative Observer Network and Weather Bureau Army Navy (WBAN) stations. The daily precipitation and temperature data from 1980 to 2010 from 11 weather stations were used from the USDA climate database. Daily solar radiation and relative humidity data obtained from the Stoneville Experiment Station at the Delta Research and Extension Center were also used as climate inputs in the model. However, the solar radiation and relative humidity data from the Stoneville Experiment Station were only available from the year 1996 to 2010. While SWAT does have a built-in weather generator to generate the missing values for solar radiation and relative humidity from 1980 to 1996, we chose to only include the climate data starting from 1996. In this way, the model can be simulated consistently without any potential differences or biases as a result of discrepancies in observed and generated solar radiation and relative humidity values. Planting and harvesting dates as well as irrigation rates in the BSRW were incorporated in the model (Table 2). The planting and harvesting dates were based on the USDA–NASS "Usual Planting and Harvesting Dates for U.S. Field Crops" for corn, soybean, cotton, and rice crops in Mississippi (USDA, 1997). The midpoint between the beginning date and final date during the most active planting and harvesting periods were used as the planting and harvesting dates in the model. Irrigation data were obtained from the Yazoo Mississippi Delta (YMD) Joint Water Management District at the

Table 2
Planting and harvesting dates and observed irrigation rates used in the model for BSRW.

Crop type	Planting date	Harvesting date	Irrigation amounts
Soybean	May 11th	October 6th	May: 30 mm June: 122 mm July: 91 mm August: 91 mm
Corn	April 10th	September 9th	May: 61 mm June: 122 mm July: 61 mm
Cotton	May 7th	October 12th	June: 61 mm July: 91 mm August: 30 mm
Rice	May 1st	September 26th	May: 305 mm June: 366 mm July: 336 mm August: 30 mm

monthly scale during the growing seasons (Table 2) (YMD, 2010). The monthly irrigation rates used in the model for corn, soybean, cotton, and rice were based on the 9 year average from 2002 to 2010 recorded by YMD Joint Water Management District. Because the irrigation rates are at the monthly scale, irrigation practices were simulated only once per month during the growing season.

2.4. Model calibration and validation procedures

Calibration and validation were conducted to assess the watershed model's performance in simulating streamflow with reasonable accuracy. The model was calibrated from 1/1/2003 to 12/31/2006 and validated from 1/1/2007 to 12/31/2009 using USGS daily streamflow data. These observed streamflow data were obtained from 3 USGS gauge stations near the towns of Merigold (USGS 07288280), Sunflower (USGS 07288500), and Leland (USGS 07288500) (Fig. 1). An auto-calibration technique was employed in this study to find a good input parameter set that allowed satisfactory model performance in simulating streamflow. The sequential uncertainty fitting (SUFI-2) algorithm, which is one of the auto-calibration programs included in the SWAT calibration and uncertainty procedures (SWAT-CUP) package, was used to find the best input parameter set to optimize the objective function. The objective function to optimize during calibration was the Nash–Sutcliffe Efficiency. The SUFI-2 program takes sources of uncertainty into account by computing r-factors and p-factors. The p-factor is the percentage of measured data in the 95% prediction uncertainty (95PPU) obtained through Latin Hypercube sampling, which can range from 0 to 1, where a p-factor of 1 indicating a perfect fit between observed and simulated data (Abbaspour, 2013). The r-factor is simply the average width of the 95PPU band divided by the standard deviation of the measured data, and this value can range from 0 to infinity (Abbaspour, 2013).

The calibration procedure required changing 12 hydrological parameters to optimize the objective function in the SUFI-2 program, which are listed in Table 3. These 12 hydrological parameters are the soil conservation service (SCS) curve number (CN2), the Manning's roughness coefficient for the main channel (CH_N2), surface runoff lag time (SURLAG), saturated hydraulic conductivity of the soil layers (mm/hr) (SOL_K), the available water capacity of the soil layer (mm H_2O/ mm soil) (SOL_AWC), the baseflow alpha factor (1/days) (ALPHA_BF), the groundwater delay time (days) (GW_DELAY), the groundwater revap coefficient (GW_REVAP), the threshold depth of water in the shallow aquifer for "revap" or percolation to the deep aquifer to occur (mm) (REVAPMN), the threshold depth of water in the shallow aquifer for baseflow to occur (mm) (GWQMN), the soil evaporation compensation factor (ESCO), and the plant uptake compensation factor (EPCO). More information on these parameters can be found in the SWAT model documentation (Neitsch et al., 2011). These parameters were chosen because they tend to be the most commonly adjusted parameters when calibrating the SWAT model for streamflow (Arnold et al., 2012; Gassman et al., 2007). Out of all the SWAT parameters to adjust for calibration, these are likely to affect the streamflow outputs the most in this particular watershed compared to other parameters that affect processes not dominant in the watershed such as snowmelt or forest canopy interception. The sampling ranges listed in Table 3 for these 12 parameters were also based on previous research using the SWAT model to calibrate for streamflow (Arnold et al., 2012; Gassman et al., 2007)

The model was simulated 1300 times to find the final values of the input parameters that yielded good statistics, namely the R^2, NSE, and RMSE statistics. A sensitivity analysis was also conducted to provide insight into which parameters had the largest effect on the simulated streamflow. Table 3 also lists the sensitivity ranking of those parameters by computing and comparing t-statistics and p-values. The t- statistic simply provides the measure of sensitivity and the *p*-value provides the significance of that sensitivity assessment. Thus, a high t-statistic value and low *p*-value indicate that the input has a large effect on the change in the model output.

In addition to streamflow, the model was also calibrated and validated for changes in water table depths at the seasonal scale. The observed water table depth data was obtained from YMD management district in the form of a shapefile containing the recorded depth measurements at hundreds of wells throughout the watershed between the years 1989 and 2010. However, the YMD management district only records the water table depths twice a year; once during the spring right before the growing season in the beginning of April and once following the end of the growing season in the beginning of October in the Mississippi Delta. To resolve this issue, a spatial calibration and validation technique was employed in this study to match simulated changes in water table depths with observed changes in water table depths at the seasonal scale. The spring and fall observed depths were spatially averaged at sub-basin 9 and also spatially averaged at sub-basin 25 (Fig. 3). The averaged water table depth values were used to calibrate and validate the model based on those two sub-basins, where sub-basin 9 was considered as the calibration area and sub-basin 25 as the validation area. The implementation of this spatial averaging technique is necessary to calibrate and validate the model for water table depths because groundwater outputs are printed at the HRU level, which do not have any spatial information. To resolve this issue, the simulated groundwater outputs were averaged at the sub-basin level. These two sub-basins were chosen because there is very little spatial variation in recorded water table depths within each of the sub-basins, and they also contain consistent observed seasonal water table depth data from 1996 to 2010. Sub-basin 9 was an area of particular interest due to the "cone of depression"

Table 3
Hydrologic parameters used in sensitivity analysis and model auto-calibration using SUFI-2.

Parameter name	Min	Max	Fitted value	*t*-Stat	*P*-value
V_CH_N2.rte	0.014	0.30	0.25	40.71	0.00
R_CN2.mgt	−10%	+10%	−1.7%	−12.07	0.00
V_SURLAG.bsn	1	12	1.39	−9.71	0.00
R_SOL_K(..). sol	−10%	+10%	−6.8%	2.21	0.03
A_GWQMN.gw	1	1000	929	1.70	0.09
A_GW_DELAY.gw	2	45	6.31	1.47	0.14
A_REVAPMN.gw	1	400	79.4	−1.25	0.21
A_GW_REVAP.gw	0.02	0.20	0.17	1.07	0.29
V_ESCO.hru	0.4	0.9	0.44	−0.76	0.45
R_SOL_AWC(..).sol	−10%	+10%	9.8%	0.32	0.75
V_EPCO.hru	0.1	0.9	0.71	−0.16	0.87
V_ALPHA_BF.gw	0.2	0.9	0.66	−0.02	0.98

Note: V_ means the existing parameter value is to be replaced by the given value, A_ means the given value is added to the existing parameter value, and R_ means the existing parameter value is multiplied by (100% plus the value). Detailed description of each parameter can be found in the SWAT documentation (Neitsch et al., 2012).

found in that area of the Mississippi Delta where land subsidence is occurring due to the over-extraction of groundwater for irrigation (Barlow and Clark, 2011).

Because the SWAT model does not print water table depths in the outputs, the changes in the water table depth between spring and fall were calculated based on the changes in water storage in the shallow aquifer. The simulated water table depth changes were obtained by multiplying the specific yield by the change in water storage in the shallow aquifer. The specific yield is simply the ratio of the volume of water that drains from a soil due to gravity to the volume of aquifer material. Therefore, the rise or decline of the water table is equal to the drainage volume, or change in water storage, divided by the specific yield. It should be noted that while the specific yield parameter is included in SWAT, it is currently not an active variable used in the SWAT source code. Therefore, we altered the specific yield parameter separately using the Solver tool in Microsoft Excel to obtain the optimal specific yield value that yielded the highest performance statistics, which are described below.

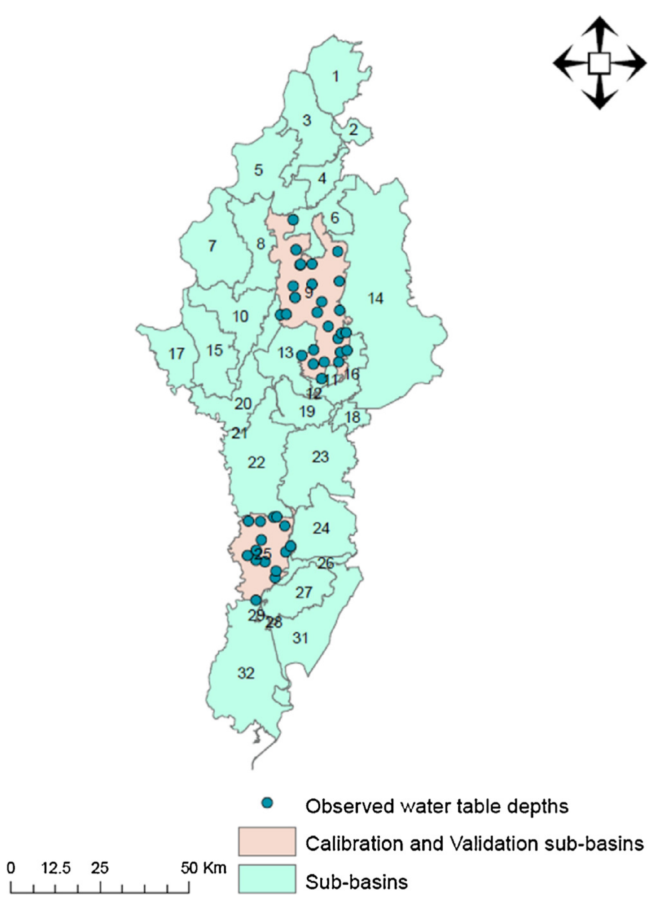

Fig. 3. Observed water table depths at sub-basins 9 and 25 were used to calibrate and validate the model for water table depths at the BSRW.

The accuracy of the model was assessed based on the coefficient of determination (R^2), Nash–Sutcliffe efficiency (NSE), and root mean square error (RMSE) statistics. The R^2 describes the proportion of variation in measured data that can be explained by the modeled data (Moriasi et al., 2007). The NSE describes how well the plot of observed data versus the modeled data fits the 1:1 line (Moriasi et al., 2007). The NSE index is a good indicator of the accuracy of the model output compared to the model input because of the index's sensitivity to extreme values in the output. The RMSE is an error index that indicates error in the squared units of the variable of interest (Moriasi et al., 2007). An RMSE of 0 indicates that there is a perfect fit between observed data and modeled data.

2.5. Model analysis and scenarios

Because previous research has demonstrated strong relationships between ET and groundwater (Ajami et al., 2011; Jayakody et al., 2013; Nachabe et al., 2005; Pandey et al., 1997), the BSRW model was analyzed to see any hydrological connections between the two hydrological parameters. The model was also simulated under 10 crop rotation scenarios, which are a combination of the four dominant crop types of corn, soybean, cotton, and rice. These scenarios include continuous corn, continuous soybean, continuous cotton, continuous rice, corn after cotton, corn after rice, corn after soybean, soybean after cotton, soybean after rice, and cotton after rice. The model scenarios were compared to the baseline to see any changes in groundwater storage and recharge that resulted from land use changes. The baseline land use condition was assumed to be the 2013 land use cover since it is impossible to capture the actual crop rotations occurring in the watershed over a long time period with reasonable accuracy. Paired two-sample *t*-tests were conducted to see if the changes in groundwater recharge and storage were significant at the 0.05 level of significance. The paired samples for the t-test consisted of the baseline scenario with a crop rotation scenario. The null hypothesis considers that there is no significant change in groundwater storage or recharge and the alternative hypothesis considers that there is a significant change in groundwater storage or recharge.

Table 4
Model performance evaluation during daily streamflow calibration and validation.

Station	Calibration			Validation				
	R^2	NSE	RMSE	R^2	NSE	RMSE	p-factor	r-factor
Merigold	0.53	0.49	24.7	0.55	0.49	21.4	0.83	1.28
Sunflower	0.60	0.59	27.2	0.64	0.63	23.2	0.80	1.31
Leland	0.68	0.66	22.2	0.75	0.72	19.4	0.87	1.35

3. Results and discussion

3.1. Model calibration and validation

The top five most sensitive parameters to streamflow with a *p*-value of less than 0.1 are Ch_N2, CN2, SURLAG, SOL_K, and GWQMN (Table 3). The CH_N2, CN2, and SURLAG parameters were the most sensitive because they dictate the amount and rate of surface runoff, which directly impacts the streamflow in the watershed. The final value chosen for CH_N2 is 0.25, which indicates that the channels are lined with rough surfaces such as dense brushes and vegetation. The final value for CN2 was changed to −1.72% of the default CN2 estimate used in the uncalibrated model. The final SURLAG value was 1.39 days, indicating a fast response time for overland flow to reach the main channels. The high sensitivity of the SOL_K and GWQMN indicate that streamflow is also heavily influenced by the movement of water in the subsurface and underground aquifer. SOL_K was changed to −6.8% of the original uncalibrated values and GWQMN was changed to 928.9 mm. The high value of GWQMN implies that the underground aquifer is unable to provide baseflow during periods of low aquifer storage and recharge. The low rates or absence of baseflow in the river channels of the BSRW usually occurs during the growing season when groundwater reserves are used for crop irrigation.

The model was calibrated for daily streamflow during a 4-year period from 1/1/2003 to 12/31/2006 and validated during a 3-year period from 1/1/2007 to 12/31/2009 at 3 USGS gage stations (Fig. 4). The R^2, NSE, RMSE, p-factors, and r-factors indicated that the model performed well in simulating streamflow and most of the peakflows were captured in the model (Table 4). During calibration, the R^2 values ranged from 0.53 to 0.68 and the NSE values ranged from 0.49 to 0.66, and during validation, the R^2 values ranged from 0.55 to 0.75 and the NSE values ranged from 0.49 to 0.72. These model evaluation statistics are consistent with previous SWAT modeling studies that use R^2 and NSE to evaluate the performance of the model during calibration and validation (Gassman et al., 2007). The p-factors ranged from 0.80 to 0.87 and the r-factors ranged from 1.28 to 1.35, which was based on the number of simulations bracketed by the 95 PPU band. It is evident that most of the 1300 simulations fell within the 95 PPU, indicating that the uncertainty in modeling streamflow was small. However, the thickness of the 95 PPU increased drastically when the model was simulating peakflows at all three gauges, which indicates a high degree of uncertainty when SWAT simulates peakflows. This also further explains why the SWAT model generally tends to underestimate high streamflows and overestimate low streamflows (Gassman et al., 2007; Jeong et al., 2010; Wu et al., 2012).

The model was also calibrated and validated for water table depth fluctuations at sub-basin 9 and sub-basin 25 (Fig. 5). The calibrated value for specific yield was found to be 0.26, which resulted in an R^2 of 0.76 and NSE of 0.71 during calibration (sub-basin 9) and R^2 of 0.86 and NSE of 0.79 during validation (sub-basin 25) (Fig. 5). The model did not perform as well in sub-basin 9, most likely due to the rapid rate of groundwater depletion in the "cone of depression" (Barlow and Clark, 2011). A specific yield of 0.26 is close to the 0.32 specific yield value chosen in previous groundwater modeling studies conducted in the Mississippi Delta region (Arthur et al., 2001; Barlow and Clark, 2011). It should be noted that this groundwater calibration process involved averaging water table depths over a large area, which reduces the spatial variation that can be captured by the model. However, this spatial averaging technique at the sub-basin level was necessary because the water table depths can only be simulated in SWAT at the HRU level, which does not have spatial information. Overall, the model performed well in simulating seasonal changes in groundwater table depths at the watershed scale.

3.2. ET and groundwater interactions

Before comparing the crop rotation scenarios, the baseline scenario was simulated at the monthly scale from 1996 to 2010 to compare the interactions of ET and groundwater within the watershed. In general, groundwater recharge rates are high during the spring months and low during the fall months (Fig. 6). The increases in groundwater recharge rates are due to the higher rainfall magnitudes that occur during the spring season that lead to increases in infiltration and percolation rates, as well as water contribution from the deep aquifer in the model. From Fig. 6, groundwater recharge start to increase rapidly in the spring seasons following the heavy precipitation events occurring in the winter seasons. However, during the summer and fall months, the alluvial aquifer does not receive much groundwater recharge, which is a result of the irrigation rates and the high transpiration rates during the growing season. Average monthly groundwater storage decreases during the summer while average monthly ET rates are high, and increases during the winter and spring when ET rates are low (Fig. 7). For example, during the months of June and July, the average monthly ET rates reached their yearly peak of 97 mm/month. These two months also experienced the largest depletion in groundwater storage by 17% for June and by 14.4% for July. In contrast, ET rates were lowest at 13.9 mm/month during December and 16.5 mm/month during January, while the average groundwater storage increased by 11.8% during December and 8.3% during January. Essentially, the alluvial aquifer is recharged during the winter and spring, and is depleted during the summer when irrigation occurs during the growing season and ET rates are high. While decreases in groundwater storage are primarily due to irrigation, groundwater storage is also lost to revap, which is dependent on ET rates. Most of the groundwater in the watershed that is lost to revap typically occurs in the months of May, June, and July, where 48% of the total annual revap takes place. Overall, ET rates played a significant role in simulating groundwater storage and groundwater recharge in the BSRW model.

It should be noted that the scheduled irrigation in the model does not necessarily reflect the actual irrigation applications practiced by farmers in the BSRW from year to year. It has been reported that the farmers in the Mississippi Delta irrigate based primarily on plant observation, which may lead the farmers to either under irrigate or over irrigate their crops (Jayakody et al., 2013). This can cause considerable spatial and temporal variations of irrigation practices throughout the watershed, especially when considering varying weather conditions. However, it is not realistic or feasible to simulate these varying irrigation applications at the watershed scale. Instead, we included the monthly average irrigation rates that have been reported by the YMD management district. Including these irrigation data in the model yielded reasonable and plausible groundwater results at the monthly scale that corresponded well with ET rates from the watershed model.

3.3. Groundwater storage and recharge

The groundwater outputs of the crop rotation scenarios were analyzed to see any significant differences in average monthly

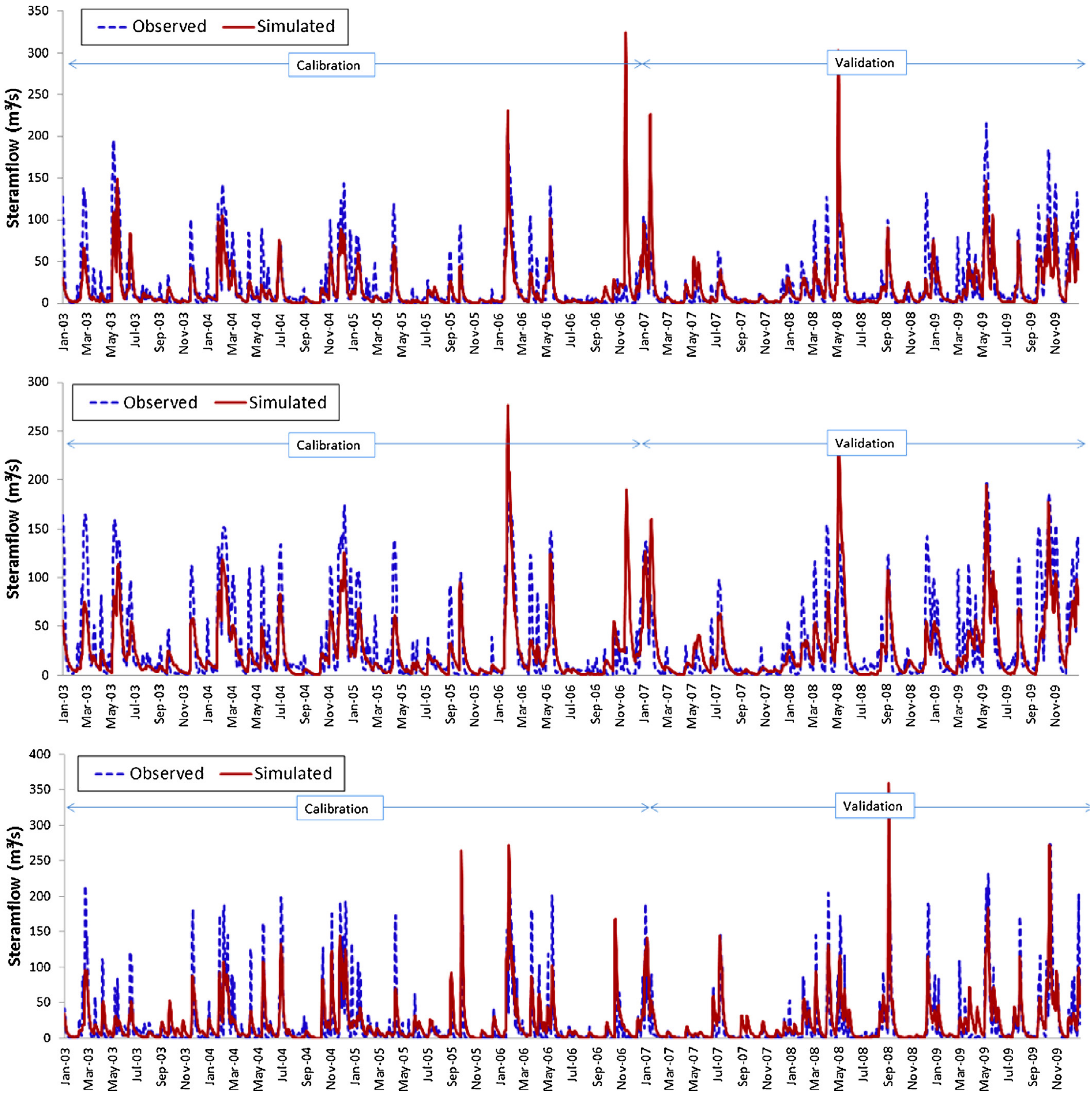

Fig. 4. Observed vs. simulated daily streamflow during model calibration (1/1/2003–12/31/2006) and validation (1/1/2007–12/31/2009) for the Merigold (USGS 07288280), Sunflower (USGS 07288500), and Leland (USGS 07288500) gauge stations in the BSRW.

groundwater recharge and storage. The model was simulated from 1996 to 2010 for each scenario, and the results of the simulations are listed in Fig. 8. Paired two-sample *t*-tests were conducted to see if the changes in groundwater recharge and storage were significant at the 0.05 level of significance (Tables 5 and 6).

Out of all the scenario simulations, continuous rice rotation leads to the greatest rates of monthly groundwater recharge (+60.1%), followed by soybean after rice (+28.1%), corn after rice (+27.7), and cotton after rice crop rotations (+19.6%) (Table 5). Continuous cotton rotation leads to the highest decreases in average monthly groundwater recharge (−17.7%), followed by corn after cotton (−10.7%), and soybean after cotton (−9.3%) (Table 5). The continuous soybean and corn after soybean crop rotations did not have a significant effect on groundwater recharge outputs in the model (Table 5). Most of the simulated crop rotation practices also had a significant effect on the average monthly groundwater storage in the shallow aquifer. The continuous corn crop rotation resulted in the largest increases in groundwater storage (+27.2%), followed by corn after cotton (+22.3%), corn after soybean (+13.3%), and continuous cotton crop rotations (+9.7%) (Table 6). Compared to baseline crop rotation, the continuous rice crop rotation resulted in the highest depletion in groundwater storage (−10.7%), followed by soybean after rice (−9.2%), and continuous soybean rotations (−9.0%) (Table 6). The soybean after cotton crop rotation scenario did not have a significant effect on the groundwater storage in the shallow aquifer (Table 6).

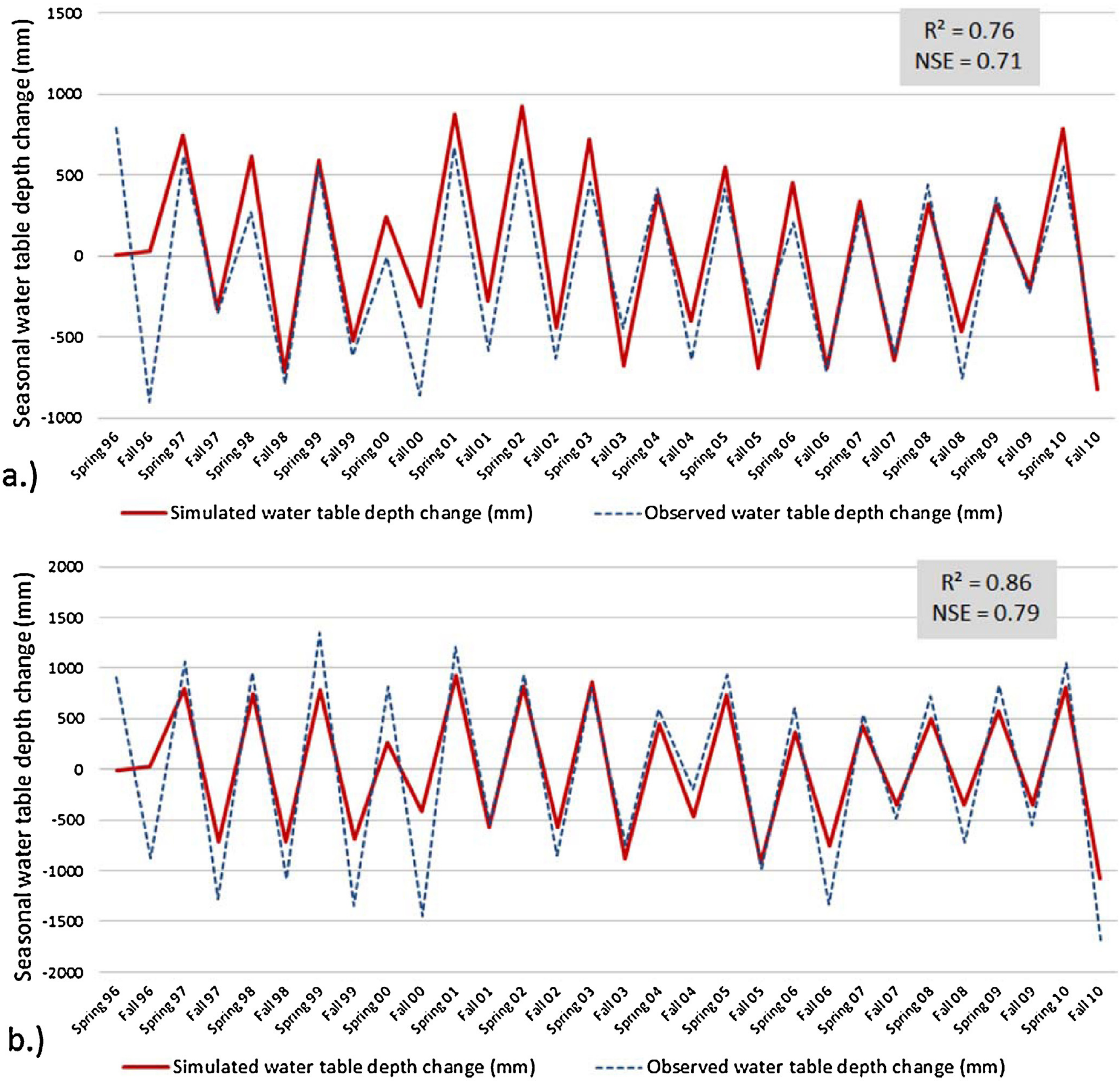

Fig. 5. Observed and simulated water table depth changes at the seasonal scale from 1996 to 2010 at the (a) calibration sub-basin and the (b) validation sub-basin.

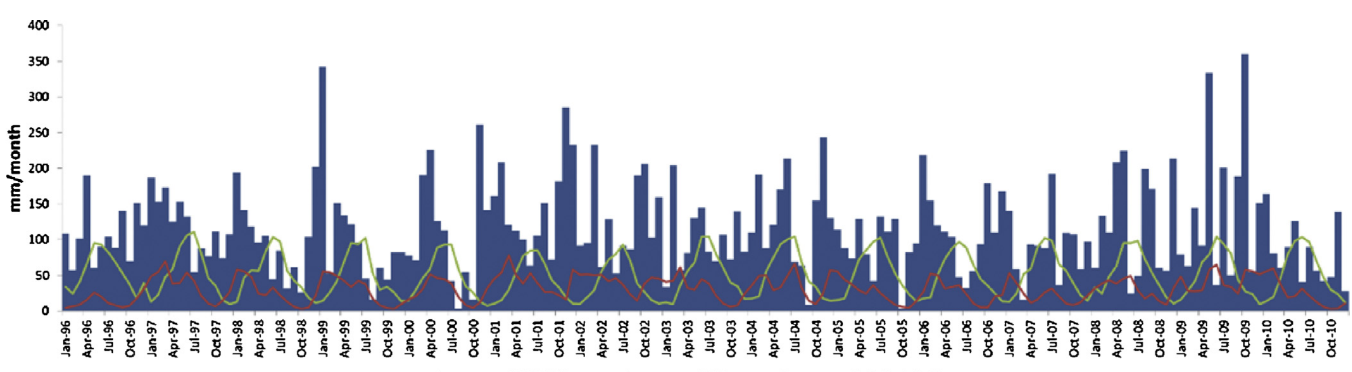

Fig. 6. Average precipitation (PRECIP), evapotranspiration (ET), and groundwater recharge (GW_RCHG) simulation from 1996 to 2010 during the baseline scenario.

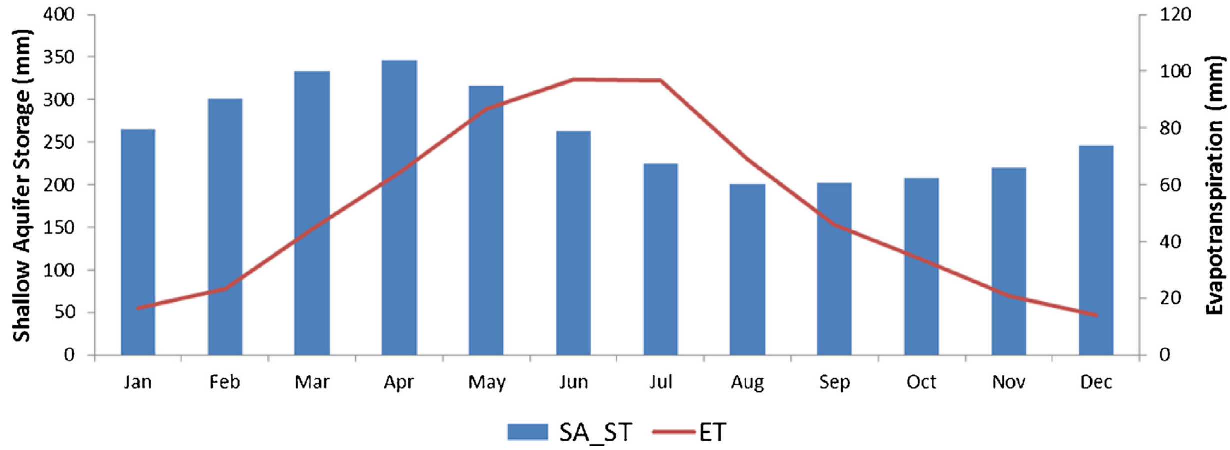

Fig. 7. Average monthly shallow aquifer storage (SA_ST) and evapotranspiration (ET) model results in the BSRW from 1996 to 2010 during the baseline scenario.

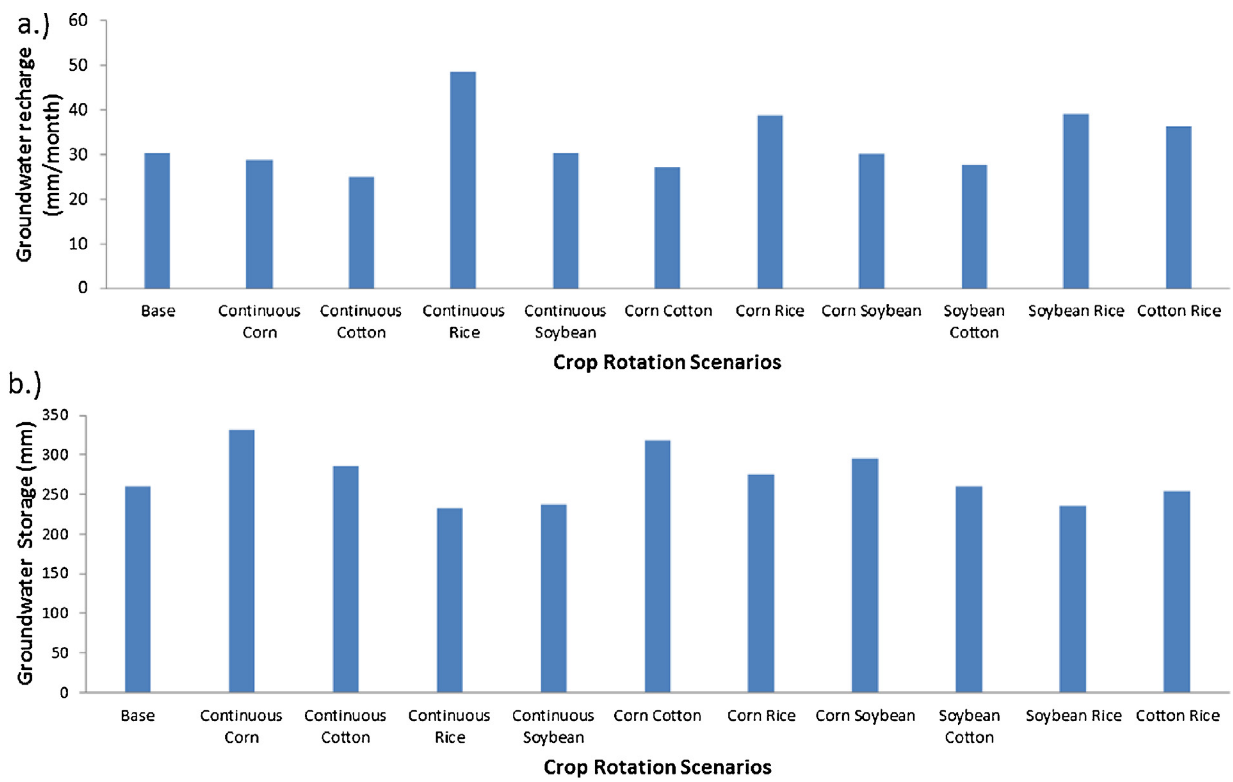

Fig. 8. Model simulated average monthly (a) groundwater recharge and (b) groundwater storage during crop rotation scenarios from 1996 to 2010 in the watershed.

The results of the crop rotation scenarios indicated that the type of crop planted in the watershed does have a potential impact on groundwater storage and recharge. All of the simulated crop rotations had varying irrigation rates, which are pumped from the alluvial aquifers. The irrigation rates caused the aquifer to respond to groundwater depletion in different ways. For example, continuous rice crop rotation caused the largest depletion of groundwater in the watershed due to the high irrigation rates (Table 2), which resulted in the highest rates of recharge. The high rates of groundwater recharge occurred in response to the deficiency of groundwater needed for irrigation. More water was allowed to recharge the aquifer under rice planting scenarios because of the shallow rooting depth of the rice crop compared to other crops, which allowed for low revap rates due to low plant root uptake during the simulation. On the other hand, the lowest recharge rates occurred during cotton planting scenarios, likely due to the deep roots of the cotton plants, which increased groundwater revap rates in the watershed. The continuous soybean and corn after soybean crop rotation scenarios had no significant effect on the groundwater recharge, which is to be expected because those are currently the most common crop rotation practices occurring in the watershed.

The corn crops caused the largest increases in shallow aquifer storage, which is to be expected due to the short time period for irrigation applications (Fig. 8). Cotton planting caused increases in groundwater storage as well, which is also the result of low irrigation rates. These results indicate that farmers and watershed managers in the BSRW should consider implementing crop rotations containing corn and cotton. Over a long period of time (>20 years), implementing these crop rotations should result in an increase in groundwater storage in the alluvial aquifer.

Table 5
The percent changes in groundwater recharge as a result of changes in crop rotation practices compared to the baseline conditions in the watershed. Paired two-sample *t*-tests were conducted to see if the changes were significant at the 0.05 level of significance.

Scenario	% Change	*t*-Value	*p*-Value
Continuous corn	−5.0	7.6	<0.01
Continuous cotton	−17.7	12.9	<0.01
Continuous rice	+60.1	−9.4	<0.01
Continuous soybean	−0.2	0.31	0.76
Corn after cotton	−10.7	9.3	<0.01
Corn after rice	27.7	−5.4	<0.01
Corn after soybean	−0.6	0.85	0.40
Soybean after cotton	−9.3	7.6	<0.01
Soybean after rice	+28.1	−5.7	<0.01
Cotton after rice	+19.6	−3.7	<0.01

Table 6
The percent changes in groundwater storage in the shallow aquifer as a result of changes in crop rotation practices compared to the baseline conditions in the watershed. Paired two-sample *t*-tests were conducted to see if the changes were significant at the 0.05 level of significance.

Scenario	% Change	*t*-Value	*p*-Value
Continuous corn	+27.2	−22.6	<0.01
Continuous cotton	+9.7	−14.5	<0.01
Continuous Rice	−10.7	7.3	<0.01
Continuous Soybean	−9.0	22.6	<0.01
Corn after cotton	+22.3	−19.9	<0.01
Corn after rice	+5.5	−5.7	<0.01
Corn after soybean	+13.3	−17.1	<0.01
Soybean after cotton	−0.1	0.2	0.85
Soybean after rice	−9.2	8.6	<0.01
Cotton after rice	−2.6	2.3	0.03

Alternatively, the rice planting scenarios resulted in the lowest groundwater storage in the alluvial aquifer, which is the result of the significantly higher irrigation rates compared to other crops. However, the rice crop scenarios resulted in the largest rates of groundwater recharge. This is interesting because while rice planting scenarios resulted in the highest rates of groundwater recharge, it was not enough to fill the shallow aquifer compared to the baseline scenario or other crop rotation scenarios. Therefore, crop rotations with rice planting should only be implemented occasionally in the watershed to allow groundwater storage to increase.

It should be noted that none of the crop rotation scenarios resulted in any significant change in evapotranspiration in the watershed. This is mostly likely the result of all the corn, cotton, rice, and soybean crops having similar transpiration rates. The change in the amount of groundwater storage was not due to the amount of baseflow in the watershed, because the threshold depth of water in the shallow aquifer for baseflow to occur (GWQMN) was set at a high value (928.9 mm) during model calibration. The storage in the shallow aquifer almost never reached 928.9 mm, so baseflow in the watershed was rare, which is in conformity with the actual physical response of the watershed (Coupe et al., 2012). The crop rotation scenarios resulted in significant changes in groundwater revap rates, which are a result of the varying plant root depths and soil evaporation rates. The changes in groundwater revap and pumping caused most of the groundwater responses in the different crop rotation simulations.

4. Conclusion

This study was conducted to develop a calibrated and validated model using SWAT for streamflow and water table depths in a humid sub- tropical climate watershed in northwestern Mississippi. The model was used to simulate any relationships between evapotranspiration and groundwater as well as simulate the effects of crop rotation strategies on groundwater storage and recharge.

The model performed well during the calibration period (R^2 = 0.53–0.68 and NSE = 0.49–0.66) and validation period (R^2 = 0.55–0.75 and NSE = 0.49–0.72) for daily streamflow, which was achieved by the SUFI-2 auto-calibration algorithm in the SWAT-CUP package. The model also performed well in simulating seasonal water table depth fluctuations at the calibration sub-basin (R^2 = 0.76 and NSE = 0.71) and at the validation sub-basin (R^2 = 0.86 and NSE = 0.79), which was achieved by setting the specific yield of the Mississippi River Valley Alluvial Aquifer to 0.26. The model was most sensitive to Manning's roughness coefficient, SCS curve number, surface runoff lag time, soil hydraulic conductivity, and the threshold shallow aquifer depth for baseflow to occur.

ET rates played a significant role in governing the amount of groundwater storage and the rate of recharge of the alluvial aquifer. The model results indicated that groundwater storage decreased during the summer months while ET rates were high, and increased during the winter and spring months when ET rates were low. The crop rotation scenarios with rice planting resulted in the lowest groundwater storage (down to −10.7%) compared to the baseline crop scenario, which is due to the high irrigation rates of the rice crop. However, the rice crop rotations resulted in the highest increases of groundwater recharge rates (up to +60.1%), likely because of the response to the deficiency of groundwater needed for irrigation as well as the limited water uptake by the shallow rice plant roots. The crop rotations with corn and cotton resulted in the largest increases in groundwater storage (+27.2%), which is the result of the low irrigation rates as well as the short time period for irrigation applications.

This study found that monthly groundwater recharge and storage were related to changes in ET rates in the BSRW in Mississippi. This study also found that implementing crop rotations that contain cotton and/or corn resulted in the largest increases in groundwater storage, and crop rotations with rice and soybean resulted in the largest decreases in groundwater storage. Farmers and watershed managers should consider the consequences of implementing certain crop rotation strategies on groundwater storage and recharge, especially in watersheds where the main source of irrigation water is from groundwater. This study should be conducted in other watersheds with different landscapes and soils to see if the resulting groundwater flows change significantly. Also, the study could be improved by incorporating future climate changes by using generated precipitation and temperature data from down-scaled global climate models.

Acknowledgements

This material is based upon work partially supported by the USDA/NIFA Grant No. 67020-21407; and National Science Foundation under Grant No. DGE-0947419 at Mississippi State University. We would like to acknowledge the support of Graduate school of the Mississippi State University, (MSU) Bagley College of Engineering at MSU. We would also like to acknowledge the support of YMD, MS for the groundwater data; USGS; and other collaborators.

References

Abbaspour, K.C., 2013. SWAT-CUP 2012: SWAT Calibration and Uncertainty Programs—A User Manual. Neprash Technology. Available at <http://www.neprashtechnology.ca/Downloads.aspx>.

Ajami, H., Meixner, T., Maddock III, T., Hogan, J.F., Guertin, D.P., 2011. Impact of land-surface elevation and riparian evapotranspiration seasonality on groundwater budget in MODFLOW models. Hydrogeol. J. 19, 1181–1188.

Arthur, J.K., 2001. Hydrogeology, model description, and flow analysis of the Mississippi river alluvial aquifer in Northwestern Mississippi. In: Water Resources Investigations Report 01–4035. Reston, Virginia, U.S. Geological Survey.

Barlow, J.R.B., Clark, B.R., 2011. Simulation of water-use conservation scenarios for the Mississippi Delta using an existing regional groundwater flow model. In: Scientific Investigations Report 2011–5019. Reston, Virginia, U.S. Geological Survey.
Batelis, S.C., Nalbantis, I., 2014. Potential effects of forest fires on streamflow in the Enipeas River Basin, Thessaly, Greece. Environ. Process. 1, 73–85.
Clark, B.R., Hart, R.M., 2009. The Mississippi Embayment Regional Aquifer Study (MERAS) —documentation of a groundwater-flow model constructed to assess water availability in the Mississippi embayment. In: Scientific Investigations Report 2009–5172. Reston, Virginia, U.S. Geological Survey.
Coupe, R.H., Barlow, J.R.B., Capel, P.D., 2012. Complexity of human and ecosystem interactions in an agricultural landscape. Environ. Dev. 4 (2012), 88–104.
Dawes, W., Ali, R., Varma, S., Emelyanova, I., Hodgson, G., McFarlane, D., 2012. Modelling the effects of climate change and cover change on groundwater recharge in south–west Western Australia. Hydrol. Earth Syst. Sci. 16, 2709–2722.
Fereres, E., Soriano, M.A., 2006. Deficit irrigation for reducing agricultural water use. J. Exp. Bot. 58 (2), 147–159.
Foley, J.A., DeFries, R., Asner, G.P., Barford, C., Bonan, G., Carpenter, S.R., Chapin, F.S., Coe, M.T., Daily, G.C., Gibbs, H.K., Helkowski, J.H., Holloway, T., Howard, E.A., Kucharik, C.J., Monfreda, C., Patz, J.A., Prentice, I.C., Ramankutty, N., Snyder, P.K., 2005. Global consequences of land use. Science 309 (5734), 570–574.
Galbiati, L., Bouraoui, F., Elorza, F.J., Bidoglio, G., 2006. Modeling the diffuse pollution loading into a Mediterranean lagoon: development and application of an integrated surface-subsurface model tool. Ecol. Model. 193 (1–2), 4–18.
Gassman, P.W., Reyes, M.R., Green, C.H., Arnold, J.G., 2007. The soil and water assessment tool: historical development, applications, and future research directions. Trans. ASABE 50 (4), 1211–1250.
Huang, T., Pang, Z., Edmunds, W.M., 2012. Soil profile evolution following land-change: implications for groundwater quantity and quality. Hydrol. Process. 27 (8), 1238–1252.
Jayakody, P., Parajuli, P.B., Sassenrath, G., Ouyang, Y., 2013. Relationships between water table & model simulated ET. Gr. Water J. 52 (2), 303–310.
Khanal, S., Parajuli, P.B., 2013. Evaluating the impacts of forest clear cutting on water and sediment yields using SWAT in Mississippi. J. Water Resour. Prot. 5 (4), 474–483.
Kim, N.W., Chung, I.M., Won, Y.S., Arnold, J.G., 2008. Development and application of the integrated SWAT-MODFLOW model. J. Hydrol. 356 (1–2), 1–16.
Konikow, L.F., 2013. Groundwater depletion in the United States (1900–2008). In: Scientific Investigations Report 2013–5079. Reston, Virginia, U.S. Geological Survey.
Lotze-Campen, H., Müller, C., Bondeau, A., Rost, S., Popp, A., Lucht, W., 2008. Global food demand, productivity growth, and the scarcity of land and water resouces: a spatially mathematical programming approach. Agric. Econ. 39 (3), 325–338.
Jeong, J., Kanna, N., Arnold, J.G., Glick, R., Gosselink, L., Srinivasan, R., 2010. Development and integration of sub-hourly rainfall-runoff modeling capability within a watershed model. Water Resour. Manag. 24 (15), 4505–4527.
Moriasi, D.N., Arnold, J.G., Vazquez-Amabile, G.G., Engel, B.A., Rossi, C.G., 2009. Incorporation of a new shallow water table depth algorithm into SWAT2005. Trans. ASABE 52 (3), 771–784.
Moriasi, D.N., Arnold, J.G., Vazquez-Amabile, G.G., Engel, B.A., 2011. Shallow water table depth algorithm in SWAT: recent developments. Trans. ASABE 54 (5), 1705–1711.
Nachabe, M., Shah, N., Ross, M., Vomacka, J., 2005. Evapotranspiration of two vegetation covers in a shallow water table environment. Soil Sci. Soc. Am. J. 69 (2), 299–492.
Narula, K.K., Gosain, A.K., 2013. Modeling hydrology, groundwater recharge and non-point nitrate loadings in the Himalayan Upper Yamuna basin. Sci. Total Environ. 468–469, S102–S116.
Neitsch, S.L., Arnold, J.G., Kiniry, J.R., Williams, J.R., 2011. Soil and water assessment tool, theoretical documentation. In: Blackland Research Center, Grassland, Soil and Water Research Laboratory. Agricultural Research Service, Temple, TX.
Pandey, R.S., Bhattacharya, A.K., Singh, O.P., Gupta, S.K., 1997. Water table draw down during drainage with evaporation/evapotranspiration. Agric. Water Manag. 35 (1–2), 61–73.
Parajuli, P.B., Jayakody, P., Sassenrath, G.F., Ouyang, Y., Pote, J.W., 2013. Assessing the impacts of crop-rotation and tillage on crop yields and sediment yield using a modeling approach. Agric. Water Manag. 119 (2013), 32–42.
Perkins, S.P., Sophocleous, M., 1999. Development of a comprehensive watershed model applied to study stream yield under drought conditions. Groundwater 37 (3), 418–426.
Roosmalen, L., Sonnenborg, T.O., Jensen, K.H., 2009. Impact of climate and land use change on the hydrology of a large-scale agricultural catchment. Water Resour. Res. 45, http://dx.doi.org/10.1029/2007WR006760.
Siebert, S., Burke, J., Faures, J.M., Frenken, K., Hoogeveen, J., Döll, P., Portmann, F.T., 2010. Groundwater use for irrigation: a global inventory. Hydrol. Earth Syst. Sci. 14, 1863–1880.
Sophocleous, M., Perkins, S.P., 2000. Methodology and application of combined watershed and ground water models in Kansas. J. Hydrol. 236 (3–4), 185–201.
Thanapakpawin, P., Richey, J., Thomas, D., Rodda, S., Campbell, B., Logsdon, M., 2006. Effects of landuse change on the hydrologic regime of the Mae Chaem river basin, NW Thailand. J. Hydrol. 334 (1–2), 215–230.
Tuppad, P., Santhi, C., Wang, X., Williams, J.R., Srinivasan, R., Gowda, P.H., 2010. Simulation of conservation practices using the APEX Model. Appl. Eng. Agric. 26 (5), 779–794.
United States Department of Agriculture, 1997. Usual planting and harvesting dates for U.S. field crops. National Agricultural Statistics Service. Agricultural Handbook Number 628.
Vazquez- Amabile, G.G., Engel, B.A., 2004. Use of SWAT to compute groundwater table depth and streamflow in the Muscatatuck River watershed. Trans. ASAE 48 (3), 991–1003.
Wang, S., Zhang, Z., McVicar, T.R., Guo, J., Tang, Y., Yao, A., 2013. Isolating the impacts of climate change and land use change on decadal streamflow variation: assessing three complementary approaches. J. Hydrol. 507 (2013), 63–74.
Wild, T.B., Davis, A.P., 2009. Simulation of the performance of a storm–water BMP. J. Environ. Eng. 135 (12), 1257–1267.
Wu, Y., Liu, S., Abdul- Aziz, O.I., 2012. Hydrological effects of the increased CO_2 and climate change in the Upper Mississippi River Basin using a modified SWAT. Climatic Change 110 (3), 977–1003.
Yazoo Mississippi Delta Joint Water Management District, 2010. 2010 Annual Work Summary. Available at <www.ymd.org> Stoneville, MS.